Inorganic Chemistry
Article

Inorg. Chem. **2011**, *50*, 1603–1613 **1603**
DOI: 10.1021/ic1020669

Long-Lived and Temperature-Independent Emission from a Novel Ruthenium(II) Complex Having an Arylborane Charge-Transfer Unit

Eri Sakuda,*,† Yuki Ando,† Akitaka Ito,† and Noboru Kitamura*,†,‡

†*Department of Chemistry, Faculty of Science,* ‡*Department of Chemical Sciences and Engineering, Graduate School of Chemical Sciences and Engineering, Hokkaido University, Sapporo 060-0810, Japan*

Received October 12, 2010

We report the redox, absorption, and emission characteristics of the tris(1,10-phenanthroline)ruthenium(II) complexes $[Ru(phen)_3]^{2+}$ bearing a (dimesityl)boryldurylethynyl (DBDE) charge-transfer (CT) unit at the 4 (**4BRu**$^{2+}$) or 5 (**5BRu**$^{2+}$) position of one of the three phen ligands. In acetonitrile at 298 K, **4BRu**$^{2+}$ showed absorption and emission maximum wavelengths at 473 and 681 nm, respectively, which were shifted to longer wavelengths by 25 and 74 nm, respectively, compared with the relevant value of **5BRu**$^{2+}$, 448 and 607 nm, respectively. The effects of a fluoride ion on the absorption and emission spectra of the complexes demonstrated that the CT interaction between the π-electron system in the phen ligand (π(aryl)) and the vacant p orbital on the boron atom (p(B)) in the DBDE group (i.e., π(aryl)−p(B) CT) participated in the excited states of the complexes in addition to the Ru(II)-to-phen metal-to-ligand CT (MLCT) interaction. Reflecting such synergistic MLCT/π(aryl)−p(B) CT, both **4BRu**$^{2+}$ and **5BRu**$^{2+}$ exhibited intense emission at 298 K with a quantum yield of 0.11. Furthermore, the emission lifetime of **4BRu**$^{2+}$ was as long as 12 μs and almost independent of the temperature (T = 280−330 K). The present study indicated that the nonemissive dd excited triplet state did not participate to nonradiative decay in the MLCT excited triplet state of **4BRu**$^{2+}$. The effects of the synergistic MLCT/π(aryl)−p(B) CT interactions on the redox, absorption/emission, and photophysical characteristics of **4BRu**$^{2+}$ and **5BRu**$^{2+}$ are discussed in detail.

Introduction

A variety of polypyridine ruthenium(II) (Ru(II)) complexes have been hitherto designed/synthesized, and their photochemical and photophysical properties were studied extensively in the past decades aiming at applications of the complexes to photosensitizers/photocatalysts in solar energy conversion systems.[1] One of the main issues of such studies is the development of a novel Ru(II) complex having a high light absorption efficiency (i.e., large molar absorption coefficient) in the visible region and a long excited-state lifetime to achieve efficient conversion of solar energy to chemical energy. For efficient utilization of solar radiation, a complex having a low-energy absorption transition(s) is preferable. Nonetheless, such a complex with a low-energy metal-to-ligand charge transfer (MLCT) absorption band and, thus, a low-energy MLCT excited triplet state (^{3}MLCT* in the energy of ν^{em}) exhibits, in general, a short excited-state lifetime (τ^{em}) because the coupling between the ^{3}MLCT* and ground-state potential surfaces for nonradiative decay increases with a lowering of the ^{3}MLCT* energy, as predicted from the energy-gap dependence of the nonradiative decay rate constant (k_{nr}): $\ln k_{nr} \propto \nu^{em}$.[2] Furthermore, the excited-state lifetime of an ordinary Ru(II) complex represented by RuL_3^{2+} [L = 2,2′-bipyridine (bpy) or 1,10-phenanthroline (phen)] shows a large temperature (T) dependence, and T elevation, in general, gives rise to a large decrease in τ^{em} owing to thermal activation from ^{3}MLCT* to the nonemitting dd excited triplet state (^{3}dd*) and subsequent fast nonradiative decay from ^{3}dd* to the ground state.[3,4] Although it has been reported that some Ru(II) complexes show T-independent τ^{em} probably due to an increase in the ^{3}MLCT*−^{3}dd* energy gap of the complex,[4] this sometimes accompanies the low-energy MLCT excited state of the

*To whom correspondence should be addressed. E-mail: sakueri@sci.hokudai.ac.jp; kitamura@sci.hokudai.ac.jp.

(1) (a) Balzani, V.; Juris, A.; Venturi, M.; Campagna, S.; Serroni, S. *Chem. Rev.* **1996**, *96*, 759. (b) Polo, A. S.; Itokazu, M. K.; Iha, N. Y. M. *Coord. Chem. Rev.* **2004**, *248*, 1343. (c) Alstrum-Acevedo, J. H.; Brennaman, M. K.; Meyer, T. L. *Inorg. Chem.* **2005**, *44*, 6802. (d) Huynh, M. H.; Dattelbaum, D. M.; Meyer, T. J. *Coord. Chem. Rev.* **2005**, *249*, 457. (e) Rau, S.; Schäfer, B.; Gleich, D.; Anders, E.; Rudolph, M.; Friedrich, M.; Görls, H.; Henry, W.; Vos, J. G. *Angew. Chem., Int. Ed.* **2006**, *45*, 6215. (f) Nazeeruddin, M. K.; Klein, C.; Liska, P.; Grätzel, M. *Coord. Chem. Rev.* **2005**, *249*, 1460. (g) Liu, F.; Concecion, J. J.; Jurss, J. W.; Cardolaccia, T.; Templeton, J. L.; Meyer, T. J. *Inorg. Chem.* **2008**, *47*, 1727. (h) Concepcion, J. J.; Jurss, J. W.; Brennaman, M. K.; Hoertz, P. G.; Patrocinio, A. O. T.; Murakami Iha, N. Y.; Templeton, J. L.; Meyer, T. J. *Acc. Chem. Res.* **2009**, *42*, 1954.

(2) (a) Caspar, J. V.; Meyer, T. J. *J. Am. Chem. Soc.* **1983**, *105*, 5583. (b) Caspar, J. V.; Meyer, T. J. *Inorg. Chem.* **1983**, *22*, 2444. (c) Allen, G. H.; White, R. P.; Rillema, D. P.; Meyer, T. J. *J. Am. Chem. Soc.* **1984**, *106*, 2613. (d) Kober, E. M.; Caspar, J. V.; Lumpkin, R. S.; Meyer, T. J. *J. Phys. Chem.* **1986**, *90*, 3722. (e) Chen, P.; Meyer, T. J. *Chem. Rev.* **1998**, *98*, 1439.

Published on Web 01/31/2011

complex and, therefore, a short τ^{em}, as predicted from the energy-gap dependence of k_{nr}. These discussions suggest that the low-energy MLCT absorption/emission and the long excited-state lifetime of a Ru(II) complex are mutually contradicting issues. One exceptional case is τ^{em} of Ru(II) having an aromatic hydrocarbon substituent(s) (ArH = pyrene, anthracene, and so forth) on the ligand, in which the thermal equilibrium between ^{3}MLCT* and the $\pi\pi^*$ excited triplet state of ArH considerably elongates τ^{em} of the complex compared with the relevant complex without ArH:[5] as an example, τ^{em} = 150 μs for RuL_3^{2+} (L = 4-pyrenylphen) in CH_3CN at 300 K.[5f] In the simple ^{3}MLCT*−^{3}dd* nonradiative decay regime, the τ^{em} value of a Ru(II) complex is limited to less than 7 μs in solution at room temperature.[6]

For synthetic modulation of the spectroscopic/photophysical properties of a transition-metal complex, we proposed in 2006 the use of a triarylborane-appended ligand.[7] The electronic structure of a triarylborane derivative is best characterized by the presence of the vacant p orbital on the boron atom (p(B)), and the CT interaction between the π orbital of the aryl group (π(aryl)) and p(B) [π(aryl)−p(B) CT] gives rise to characteristic spectroscopic and photophysical properties of the derivative as a represented example, being those of tri-9-anthrylborane and other derivatives.[8] By introduction of a triarylborane substituent to the ligand of a transition-metal complex, one may expect synergistic interactions between the π(aryl)−p(B) CT in the triarylborane unit and MLCT in the transition-metal complex, realizing novel spectroscopic and photophysical functions, not obtained by the triarylborane or metal complex alone. In practice, we succeeded in the synthetic tuning of the emission quantum yield (Φ^{em}) and lifetime of a 2,2′:6′,2″-terpyridineplatinum(II) (tpy = 2,2′:6′,2″-terpyridine) complex by introduction of a (dimesityl)phenylborane group at the 4′ position of tpy, B-tpy: $[Pt(B\text{-}tpy)Cl]^+$, Φ^{em} = 0.011, and τ^{em} = 0.6 μs in $CHCl_3$ at room temperature.[7] Because it has been known that $[Pt(tpy)Cl]^+$ in solution at room temperature is nonluminescent,[9] introduction of the triarylborane CT unit remarkably influences the photophysical properties of the $[Pt(B\text{-}tpy)Cl]^+$ complex. After our first report on $[Pt(B\text{-}tpy)Cl]^+$, several research groups reported transition-metal (Pt(II),[10] Ir(III),[11] Ru(II),[12] Re(I),[13] or Cu(I)[10a,b]) complexes bearing an arylborane unit(s) on the ligand, and some of the complexes are shown to be luminescent in solution at room temperature.[10b−d,11,13] Nonetheless, detailed experiments on the photophysical properties of the complexes bearing an arylborane unit(s) have not been reported yet: T dependences of the emission spectrum and τ^{em}, radiative/nonradiative rate constants, and so forth. We anticipate that synergistic MLCT/π(aryl)−p(B) CT interactions can tune the spectroscopic and photophysical properties of various transition-metal complexes.

In this Article, we report here that the Ru(II) complex bearing a (dimesityl)borylduryletheynyl (DBDE) group at the 4 (**4BRu**$^{2+}$) or 5 (**5BRu**$^{2+}$) position of a 1,10-phenanthroline ligand shows quite intriguing spectroscopic and photophysical properties: see Chart 1 for the structures. In particular, we found that **4BRu**$^{2+}$ exhibited essentially a low-energy and T-independent emission in solution with Φ^{em} = 0.11 and τ^{em} = 12 μs. To the best of our knowledge, the τ^{em} value of **4BRu**$^{2+}$ is the longest among those of the polypyridine ruthenium(II) complexes hitherto reported. The synthesis and redox, spectroscopic, and photophysical properties of **4BRu**$^{2+}$ and

(3) (a) Van Houten, J.; Watts, R. J. *J. Am. Chem. Soc.* **1976**, *98*, 4853. (b) Van Houten, J.; Watts, R. J. *Inorg. Chem.* **1978**, *17*, 3381. (c) Durham, B.; Caspar, J. V.; Nagle, J. K.; Meyer, T. J. *J. Am. Chem. Soc.* **1982**, *104*, 4803. (d) Barrigelletti, F.; Juris, A.; Balzani, V.; Belser, P.; von Zelewsky, A. *J. Phys. Chem.* **1987**, *91*, 1095. (e) Juris, A.; Balzani, V.; Barrigelletti, F.; Campagna, S.; Belser, P.; von Zelewsky, A. *Coord. Chem. Rev.* **1988**, *84*, 85. (f) Ferrando, S. R. L.; Maheroot, U. S. M.; Deshayes, K. D.; Kinstle, T. H.; Ogawa, M. Y. *J. Am. Chem. Soc.* **1996**, *118*, 5783. (g) Macatangay, A.; Zheng, G. Y.; Rillema, D. P.; Jackman, D. C.; Merkert, J. W. *Inorg. Chem.* **1996**, *35*, 6823. (h) Zheng, G. Y.; Rillema, D. P. *Inorg. Chem.* **1996**, *35*, 7118. (i) Hammarström, L.; Alsins, J.; Börje, A.; Norrby, T.; Zhang, L.; Åkermark, B. *J. Photochem. Photobiol. A: Chem.* **1997**, *102*, 139. (j) Hammarström, L.; Barigelletti, F.; Flamigni, L.; Indelli, M. T.; Armaroli, N.; Calogero, G.; Guardigli, M.; Sour, A.; Collin, J.-P.; Sauvage, J.-P. *J. Phys. Chem. A* **1997**, *101*, 9061. (k) Wu, F.; Riesgo, E.; Paualora, A.; Kipp, R. A.; Schmehl, R. H.; Thummel, R. P. *Inorg. Chem.* **1999**, *38*, 5620. (l) Benniston, A. C.; Chapman, G.; Harriman, A.; Mehrabi, M.; Sams, C. A. *Inorg. Chem.* **2004**, *43*, 4227. (m) Thompson, D. W.; Fleming, C. N.; Myron, B. D.; Meyer, T. J. *J. Phys. Chem. B* **2007**, *111*, 6930. (n) Abrahamsson, M.; Becker, H.-C.; Hammarström, L.; Bonnefous, C.; Chamchoumis, C.; Thummel, R. P. *Inorg. Chem.* **2007**, *46*, 10354.

(4) (a) Allen, G. H.; White, R. P.; Rillema, D. P.; Meyer, T. J. *J. Am. Chem. Soc.* **1984**, *106*, 2613. (b) Henderson, L. J., Jr.; Cherry, W. R. *J. Photochem.* **1985**, *28*, 143. (c) Wacholtz, W. F.; Auerbach, R. A.; Schmehl, R. H. *Inorg. Chem.* **1986**, *25*, 227. (d) Kawanishi, Y.; Kitamura, N.; Tazuke, S. *Inorg. Chem.* **1989**, *28*, 2968. (e) Wang, Y.; Peres, W.; Zheng, G. Y.; Rillema, D. P. *Inorg. Chem.* **1998**, *37*, 2051. (f) Rillema, D. P.; Blanton, C. B.; Shaver, R. J.; Jackman, D. C.; Boldaji, M.; Bundy, S.; Worl, L. A.; Meyer, T. J. *Inorg. Chem.* **1992**, *31*, 1600. (g) Treadway, J. A.; Loeb, B.; Lopez, R.; Anderson, P. A.; Keene, F. R.; Meyer, T. J. *Inorg. Chem.* **1996**, *35*, 2242. (h) Zheng, G. Y.; Wang, Y.; Rillema, D. P. *Inorg. Chem.* **1996**, *35*, 7118. (i) Wang, Y.; Greg, W. P.; Zheng, G. Y.; Rillema, D. P. *Inorg. Chem.* **1998**, *37*, 2051.

(5) (a) Simon, J. A.; Curry, S. L.; Schmehl, R. H.; Schatz, T. R.; Piotrowiak, P.; Jin, X.; Thummel, R. P. *J. Am. Chem. Soc.* **1997**, *119*, 11012. (b) Harriman, A.; Hissler, M.; Khatyr, A.; Ziessel, R. *Chem. Commun.* **1999**, 735. (c) Tyson, D. S.; Castellano, F. N. *J. Phys. Chem. A* **1999**, *103*, 10955. (d) Michalec, J. F.; Behune, S. A.; McMillin, D. R. *Inorg. Chem.* **2000**, *39*, 2708. (e) Tyson, D. S.; Bialecki, J.; Castellano, F. N. *Chem. Commun.* **2000**, 2355. (f) Tyson, D. S.; Henbest, K. B.; Bialecki, J.; Castellano, F. N. *J. Phys. Chem. A* **2001**, *105*, 8154. (g) Morales, A. F.; Accorsi, G.; Armaroli, N.; Barigelletti, F.; Pope, S. J. A.; Ward, M. *Inorg. Chem.* **2002**, *41*, 6711. (h) Maubert, B.; MaClenagham, N. D.; Indelli, M. T.; Campagna, S. *J. Phys. Chem. A* **2003**, *107*, 447. (i) Pomestchenko, I. E.; Luman, C. R.; Hissler, M.; Ziessel, R.; Castellano, F. N. *Inorg. Chem.* **2003**, *42*, 1394. (j) Benniston, A. C.; Harriman, A.; Lawwrie, D. J.; Mayeux, A. *Phys. Chem. Chem. Phys.* **2004**, *6*, 51. (k) Wang, X.-Y.; Del Guerzo, A.; Schmehl, R. H. *J. Photochem. Photobiol. C: Rev.* **2004**, *5*, 55. (l) Kozlov, D. V.; Tyson, D. S.; Goze, C.; Ziessel, R.; Castellano, F. N. *Inorg. Chem.* **2004**, *43*, 6083–6092. (m) Balazs, G. C.; del Guerzo, A.; Schmehl, R. H. *Photochem. Photobiol. Sci.* **2005**, *4*, 89. (n) Gu, J.; Chen, J.; Schmehl, R. H. *J. Am. Chem. Soc.* **2010**, *132*, 7338.

(6) Montalti, M.; Credi, A.; Prodi, L.; Gandolfi, M. T. *Handbook of Photochemistry*, 3rd ed.; Taylor & Francis: Boca Raton, FL, 2006.

(7) Sakuda, E.; Funahashi, A.; Kitamura, N. *Inorg. Chem.* **2006**, *45*, 10670.

(8) (a) Kitamura, N.; Sakuda, E. *J. Phys. Chem. A* **2005**, *109*, 7429. (b) Kitamura, N.; Sakuda, E.; Yoshizawa, T.; Iimori, T.; Ohta, N. *J. Phys. Chem. A* **2005**, *109*, 7435. (c) Sakuda, E.; Tsuge, K.; Sasaki, Y.; Kitamura, N. *J. Phys. Chem. B* **2005**, *109*, 22326. (d) Kitamura, N.; Sakuda, E.; Iwahashi, Y.; Tsuge, K.; Sasaki, Y.; Ishizaka, S. *J. Photochem. Photobiol. A: Chem.* **2009**, *207*, 102. (e) Kitamura, N.; Sakuda, E.; Ando, E. *Chem. Lett.* **2009**, *38*, 938. (f) Sakuda, E.; Ando, Y.; Ito, A.; Kitamura, N. *J. Phys. Chem. A* **2010**, *114*, 9144.

(9) Aldridge, T. K.; Stacy, E. M.; McMillin, D. R. *Inorg. Chem.* **1994**, *33*, 722.

(10) (a) Sun, Y.; Ross, N.; Zhao, S. B.; Huszarik, K.; Jia, W.-L.; Wang, R.-Y.; Macartney, D.; Wang, S. *J. Am. Chem. Soc.* **2007**, *129*, 7510. (b) Zhao, S.-B.; M^{c}Cormick, T.; Wang, S. *Inorg. Chem.* **2007**, *46*, 10965. (c) Sun, Y.; Wang, S. *Inorg. Chem.* **2009**, *48*, 3755. (d) Hudson, Z. M.; Zhao, S.-B.; Wang, R.-Y.; Wang, S. *Chem.—Eur. J.* **2009**, *15*, 6131. (e) Rao, Y.-L.; Wang, S. *Inorg. Chem.* **2009**, *48*, 7698. (f) Sun, Y.; Wang, S. *Inorg. Chem.* **2010**, *49*, 4394.

(11) (a) Zhou, G.; Ho, C.-L.; Wong, W.-Y.; Wang, Q.; Ma, D.; Wang, L.; Lin, Z.; Marder, T. B.; Beeby, A. *Adv. Funct. Mater.* **2008**, *18*, 499. (b) You, Y.; park, S. Y. *Adv. Mater.* **2008**, *20*, 3820. (c) Zhao, Q.; Li, F.; Liu, S.; Yu, M.; Liu, Z.; Yi, T.; Huang, C. *Inorg. Chem.* **2008**, *47*, 9256.

(12) Wade, C. R.; Gabbaï, F. P. *Inorg. Chem.* **2010**, *49*, 714.

(13) Lam, S.-T.; Zhu, N.; Yam, V. W.-W. *Inorg. Chem.* **2009**, *48*, 9664.

Chart 1. Structures of $\mathbf{4BRu^{2+}}$ and $\mathbf{5BRu^{2+}}$

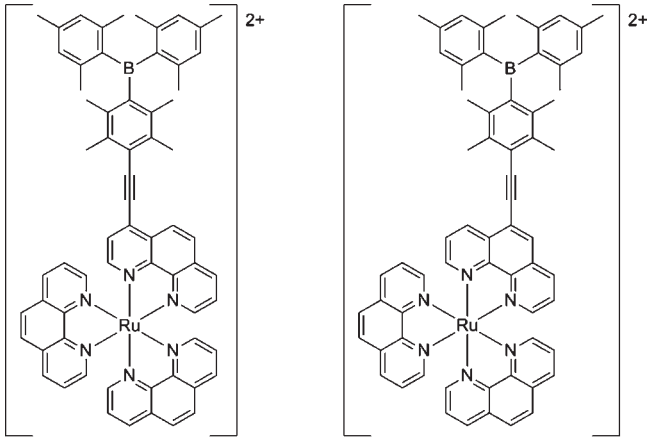

$\mathbf{4BRu^{2+}}$ $\mathbf{5BRu^{2+}}$

$\mathbf{5BRu^{2+}}$ are reported in detail, and the origin of the long-lived and *T*-independent emission lifetime of $\mathbf{4BRu^{2+}}$ is discussed.

Experimental Section

Synthesis of $\mathbf{4BRu^{2+}}$ and $\mathbf{5BRu^{2+}}$. The synthetic routes to $\mathbf{4BRu^{2+}}$ and $\mathbf{5BRu^{2+}}$ are shown in Chart 2. $\mathbf{4BRu^{2+}}$ was synthesized by the Sonogashira−Hagiwara cross-coupling reaction between (ethynylduryl)dimesitylborane (EDDB) and a PF_6 salt of $[Ru(phen)_2(4\text{-Br-phen})]^{2+}$. EDDB was synthesized according to the literature,[14] and $[Ru(phen)_2(4\text{-Br-phen})]^{2+}$ was prepared by the reaction between *cis*-dichlorobis(1,10-phenanthroline)ruthenium(II) (*cis*-$Ru(phen)_2Cl_2$)[15] and 4-Br-phen.[16,17] $\mathbf{5BRu^{2+}}$ was synthesized by reacting $[Ru(phen)_2(5\text{-ethynylphen})](PF_6)_2$ with (iododuryl)dimesitylborane (IDDB) in the presence of dichlorobis(triphenylphosphine)palladium(II) [$Pd(PPh_3)_2Cl_2$] and CuI.

All of the chemicals used for the synthesis of $\mathbf{4BRu^{2+}}$ and $\mathbf{5BRu^{2+}}$, purchased from Wako Pure Chemical Ind., Kanto Chemical Co. Inc., Tokyo Kasei Kogyo Co. Ltd., or Sigma-Aldrich Co., were used as supplied. Column chromatography was carried out by using Merck silica gel 60 (particle size 0.063−0.200 mm) or GE Healthcare Sephadex LH-20.

^{1}H NMR spectra were recorded on a JEOL JME-EX270 FT-NMR system (270 MHz). The chemical shifts of the spectra determined in $CDCl_3$ or CD_3CN were given in ppm, with tetramethylsilane being an internal standard (0.00 ppm). Electrospray ionization mass spectometry (ESI-MS) spectra were recorded on a Waters micromass ZQ spectrometer.

Synthesis of $[Ru(phen)_2\{4\text{-(dimesitylborylduryl ethynyl)-phen}\}]^{2+}PF_6$ Salt: $\mathbf{4BRu^{2+}}$. Synthesis of $[Ru(phen)_2(4\text{-Br-phen})]^{2+}PF_6$ Salt. A suspension of *cis*-$Ru(phen)_2Cl_2$ (60 mg, 0.11 mmol)[15] and 4-Br-phen[16,17] (37 mg, 0.14 mmol) in ethylene glycol (8 mL) was purged with an N_2 gas stream for 15 min. Upon microwave irradiation (200 W), the reaction mixture became a homogeneous solution. After microwave irradiation for 2 min, the reaction mixture was allowed to cool to ambient temperature and a saturated aqueous KPF_6 solution was added dropwise to the solution, giving red precipitates. The precipitates were collected by suction filtration, affording $[Ru(phen)_2(4\text{-Br-phen})](PF_6)_2$ as red solids (100 mg, 88%). ESI-MS: *m*/*z* 361 ($[M - 2PF_6]^{2+}$).

Synthesis of $\mathbf{4BRu^{2+}}PF_6$ Salt. After an oven-dried Schlenk tube was evacuated and filled with an Ar gas, $[Ru(phen)_2(4\text{-Br-phen})](PF_6)_2$ (78 mg, 0.078 mmol), CuI (1.8 mg, 0.0094 mmol), and $Pd(PPh_3)_2Cl_2$ (3.3 mg, 0.0046 mmol) were added, and the tube was evacuated and filled with an Ar gas. An Ar-gas-purged CH_3CN (2.2 mL)/triethylamine (1 mL) mixture was added to the tube and stirred for 15 min at room temperature. A tetrahydrofuran (THF; 1.6 mL) solution of EDDB (40 mg, 0.098 mmol) was then added dropwise to the reaction mixture. The mixture was stirred at 50 °C for 2.5 h under a N_2 gas atmosphere and then cooled to ambient temperature. The insoluble solids were removed by filtration through Celite, and the concentrated filtrate was added dropwise to a sufficient amount of a CH_3CN/*n*-hexane mixture, giving red precipitates. The crude product was purified by column chromatography (LH-20, ethanol/CH_3CN = 1/1 (v/v)). The product was dissolved in a CH_3CN/H_2O mixture (1/1 (v/v)), and then diethyl ether was added to the mixture. The organic layer was separated, washed with water, and evaporated under reduced pressure, affording a PF_6 salt of $\mathbf{4BRu^{2+}}$ as red solids (51 mg, 50%). ^{1}H NMR (270 MHz, CD_3CN): δ 1.95 (s, 12H), 2.04 (s, 6H), 2.52 (s, 6H), 6.81 (s, 4H), 7.61−7.68 (m, 5H), 7.73 (d, 1H, J = 5.6 Hz), 8.02−8.08 (m, 5H), 8.12 (dd, 1H, J = 0.92 and 5.2 Hz), 8.26 (s, 4H), 8.35 (d, 1H, J = 9.6 Hz), 8.59−8.65 (m, 6H). Anal. Calcd for $C_{66}H_{57}BF_{12}N_6P_2Ru \cdot H_2O$: C, 58.54; H, 4.39; N, 6.21. Found: C, 58.68; H, 4.49; N, 6.05. ESI-MS: *m*/*z* 523 ($[M - 2PF_6]^{2+}$).

Synthesis of $[Ru(phen)_2\{5\text{-(dimesitylborylduryl ethynyl)-phen}\}]^{2+}PF_6$ Salt: $\mathbf{5BRu^{2+}}$. Synthesis of 5-Ethynyl-1,10-phenanthroline (5-E-phen).[18] 5-Bromo-1,10-phenanthroline (1.0 g, 3.9 mmol) prepared by the reported method[19] was dissolved in 50 mL of THF, and the solution was purged with an Ar gas stream for 10 min at room temperature. Into the mixture were added (trimethylsilyl)acetylene (0.85 mL, 6.0 mmol), diisopropylamine (5 mL, 35 mmol), $Pd(PPh_3)_2Cl_2$ (250 mg, 0.36 mmol), and CuI (83 mg, 0.44 mmol), and the mixture under an Ar gas atmosphere was heated at reflux temperature for 7 h under stirring. After cooling to room temperature, insoluble solids were filtered off and the filtrate was evaporated to dryness. The residues were dispersed in an aqueous KCN (200 mg, 20 mL)/CH_3OH (50 mL) mixture, and the suspension was treated by ultrasonic irradiation for 1 h. The solution was extracted with $CHCl_3$ (50 mL) three times, and the combined $CHCl_3$ solution dried over Na_2SO_4 was evaporated to dryness. The crude product was purified successively by flash column chromatography (SiO_2, CH_2Cl_2/CH_3OH = 95/5 (v/v)) and recrystallization from a CH_2Cl_2/*n*-hexane mixture, yielding 5-E-phen as off-white solids (0.39 g, 49%).

Synthesis of $[Ru(phen)_2(5\text{-E-phen})]^{2+}PF_6$ Salt. An ethanol solution (100 mL) of 5-E-phen (100 mg, 0.49 mmol) and *cis*-$Ru(phen)_2Cl_2$ (250 mg, 0.47 mmol) under an Ar gas atmosphere was heated at reflux temperature for 7 h under stirring. After cooling to room temperature, the solvent was evaporated to dryness. The residues were dissolved in a minimum amount of water, and to the solution was added dropwise a concentrated aqueous NH_4PF_6 solution. The precipitated solids were collected by suction filtration and washed successively with water and an acetone/diethyl ether mixture. After drying in vacuum, the crude product was purified successively by flash column chromatography (Al_2O_3 and CH_3CN) and recrystallization from an acetone/ethanol/*n*-hexane mixture, yielding $[Ru(phen)_2(5\text{-E-phen})](PF_6)_2$ as red solids (0.27 g, 58%). ^{1}H NMR (270 MHz, CD_3CN): δ 4.13 (s, 1H), 7.65 (m, 7H), 8.04 (m, 6H), 8.25 (s, 4H), 8.55 (m, 5H), 8.85 (d, 2H, J = 8.3 Hz). Anal. Calcd for $C_{38}H_{24}N_6P_2F_{12}Ru$: C, 47.76; H, 2.53; N, 8.79. Found: C, 47.76; H, 2.84; N, 8.54.

(14) Yamaguchi, S.; Shirasaka, T.; Tamao, K. *Org. Lett.* **2000**, *2*, 4129.
(15) Sprintschnik, G.; Sprintschnik, H. W.; Kirsch, P. P.; Whitten, D. G. *J. Am. Chem. Soc.* **1977**, *99*, 4947.
(16) Poe, D. P.; Eppen, A. D.; Whoolery, S. P. *Talanta* **1980**, *27*, 368.
(17) Bijeire, L.; Legentil, L.; Bastide, J.; Darro, F.; Rochart, C.; Delfourne, E. *Eur. J. Org. Chem.* **2004**, 1981.
(18) Ziessel, R.; Suffert, J.; Youinou, M.-T. *J. Org. Chem.* **1996**, *61*, 6535.
(19) Hissler, M.; Connick, W. B.; Geiger, D. K.; McGarrah, J. E.; Lipa, D.; Lachicotte, R. J.; Eisenberg, R. *Inorg. Chem.* **2000**, *39*, 447.

Chart 2. Synthetic Routes to $\mathbf{4BRu^{2+}}$ and $\mathbf{5BRu^{2+}}$

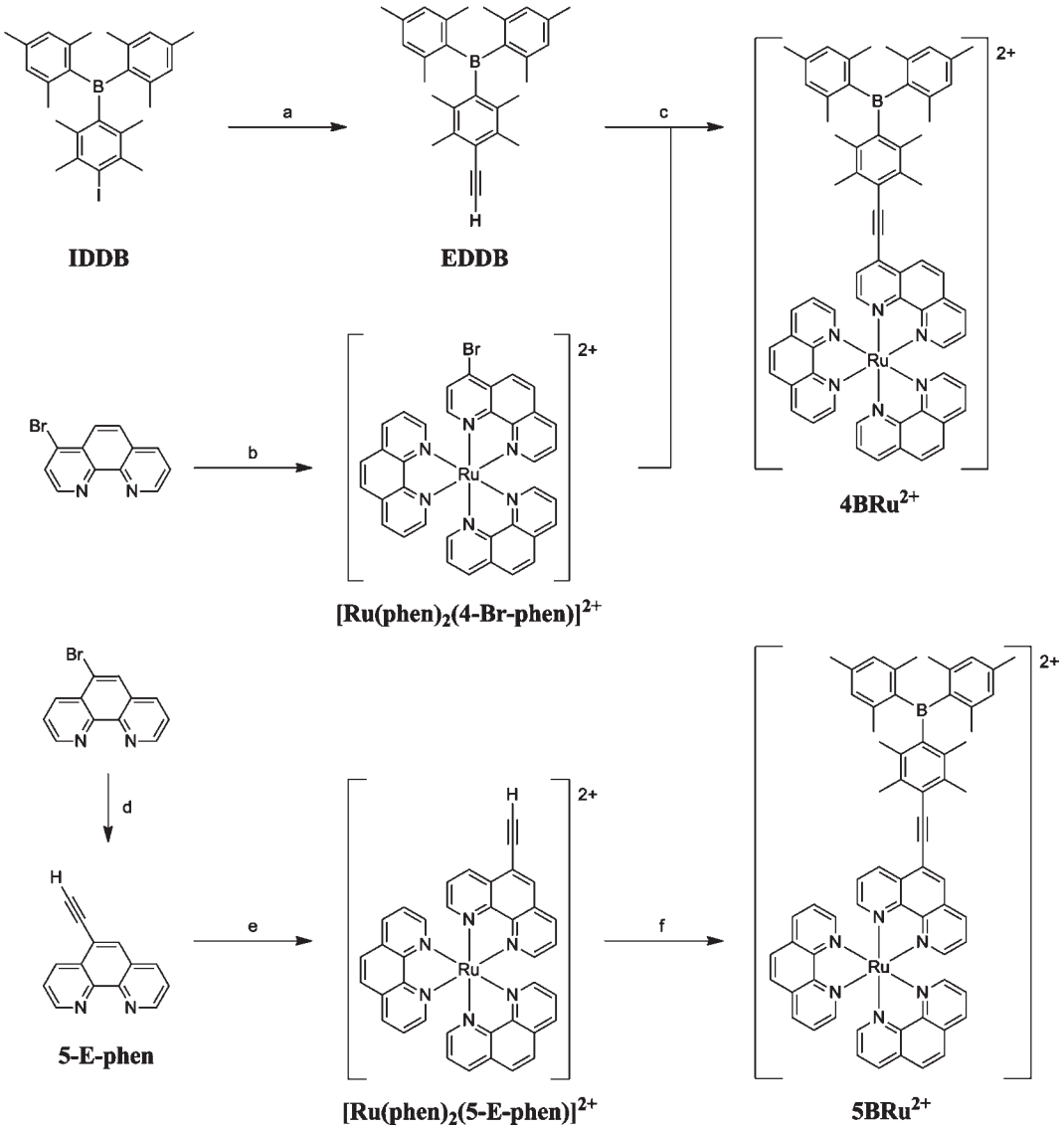

(a) (1) (Trimethylsilyl)acetylene, $Pd(PPh_3)_2Cl_2$, CuI, Et_2NH, reflux, 18 h; (2) KOH, MeOH/THF, rt, 12 h. (b) *cis*-$[Ru(phen)_2Cl_2]$, ethylene glycol, MW (200 W), 2 min, and then KPF_6. (c) $Pd(PPh_3)_2Cl_2$, CuI, NEt_3, CH_3CN/THF, 50 °C, 2.5 h. (d) (1) (Trimethylsilyl)acetylene, $Pd(PPh_3)_2Cl_2$, CuI, Et_2NH, reflux, 18 h; (2) KCN, MeOH, sonication, 1 h. (e) *cis*-$[Ru(phen)_2Cl_2]$, EtOH, reflux, 7 h, and then KPF_6. (f) IDDB, $Pd(PPh_3)_2Cl_2$, CuI, NEt_3, CH_3CN/THF, 70 °C, 15 h.

Synthesis of $\mathbf{5BRu^{2+}PF_6}$ Salt. After an oven-dried Schlenk tube was evacuated and filled with an Ar gas, IDDB (180 mg, 0.36 mmol), CuI (6.4 mg, 0.034 mmol), and $Pd(PPh_3)_2Cl_2$ (13 mg, 0.018 mmol) were added, and the tube was evacuated and filled with an Ar gas. An Ar-gas-purged THF (4 mL)/triethylamine (3 mL) solution was added to the tube and stirred at room temperature for 15 min. After CH_3CN (ca. 1 mL) was added to the mixture, a CH_3CN (5.5 mL) solution of $[Ru(phen)_2(5\text{-E-phen})](PF_6)_2$ (290 mg, 0.30 mmol) was added dropwise, and the resultant solution was heated at 70 °C for 15 h under a N_2 gas atmosphere. After the reaction, the mixture was filtered through Celite and the filtrate was evaporated to dryness under reduced pressure. The residues were dissolved in a minimum amount of acetone, and the product was reprecipitated in *n*-hexane. The precipitates collected by suction filtration were purified by column chromatograpy (LH-20, ethanol/CH_3CN = 1/1 (v/v)). After evaporation of the eluted solution under reduced pressure, the product was dissolved in a CH_3CN/H_2O mixture (1/1 (v/v)), and then diethyl ether was added to the mixture. The organic layer was separated, washed with water, and evaporated to dryness under reduced pressure, affording a PF_6 salt of $\mathbf{5BRu^{2+}}$ as orange solids (113 mg, 28%). ^1H NMR (270 MHz, CD_3CN): δ 1.95 (s, 12H), 2.06 (s, 6H), 2.25 (s, 6H), 6.81 (s, 4H), 7.59−7.67 (m, 5H), 7.71 (dd, 1H, J = 5.3 and 8.4 Hz), 8.00−8.08 (m, 6H), 8.25 (s, 4H), 8.55 (t, 2H, J = 4.2 Hz), 8.60 (dd, 4H, J = 1.2 and 2.5 Hz), 8.95 (d, 1H, J = 1.1 and 8.4 Hz). Anal. Calcd for $C_{66}H_{57}BF_{12}N_6P_2Ru \cdot H_2O$: C, 58.16; H, 4.44; N, 6.16. Found: C, 58.14; H, 4.39; N, 5.98. ESI-MS: m/z 523 ($[M - 2PF_6]^{2+}$).

Spectroscopic and Electrochemical Measurements. Solvents for spectroscopic and electrochemical measurements were distilled prior to the use.[20] Absorption and corrected emission spectra of $\mathbf{4BRu^{2+}}$, $\mathbf{5BRu^{2+}}$, and $Ru(phen)_3^{2+}$ were measured by using a Hitachi UV-3300 spectrophotometer and a Hamamatsu multichannel photodetector (PMA-11, excitation wavelength = 355 nm), respectively. The absolute emission quantum yields (Φ^{em}) of the complexes were measured by a Hamamatsu C9920-02

(20) Perrin, D. D.: Armarego, W. L. F.; Perrin, D. R. *Purification of Laboratory Chemicals*, 2nd ed.; Pargamon Press: New York, 1980.

system equipped with an integrating sphere and a red-sensitive multichannel photodetector (PMA-12, excitation wavelength = 450 nm).[21] The absorbance of a sample solution was set at < 0.05 at the excitation wavelength. Emission lifetime measurements were conducted by using a streak camera (Hamamatsu Photonics, C4334) as a photodetector at 355 nm excitation (LOTIS TII Ltd., 355 nm). A liquid N_2 cryostat (DN1704 optical Dewar and 3120 temperature controller, Oxford Instruments) was used to control the sample temperature. For emission spectroscopy, sample solutions were deaerated by purging an Ar gas stream over 30 min.

Cyclic voltammetry was conducted by using an electrochemical analyzer (BAS, ALS-701A). The concentrations of the Ru(II) complexes in *N*,*N*-dimethylformamide (DMF) were set at 5×10^{-4} mol dm^{-3} (= M), and 0.1 M tetra-*n*-butylammonium hexafluorophosphate ($TBAPF_6$) was used as a supporting electrolyte. Sample solutions were deaerated by purging an Ar gas stream over 20 min prior to the experiments. A three-electrode system was employed by using Pt working, Pt auxiliary, and saturated calomel electrode (SCE) reference electrodes.

Theoretical Calculations. The calculations on the electron densities in the highest occupied molecular orbital (HOMO)/lowest unoccupied molecular orbital (LUMO) levels of **4BRu**$^{2+}$ and **5BRu**$^{2+}$ were conducted on the *Gaussian 09W* programs.[22] Optimizations of the structures of the complexes were performed by using the B3LYP density functional theory (DFT). The LANL2DZ and 6-31* basis sets were used to treat the ruthenium atom and all other atoms, respectively. Time-dependent DFT (TD-DFT) calculations were then performed to estimate the energies and oscillator strengths of the 10 lowest-energy transitions. The contours of the electron density were plotted by using Chem3D 11.0.

Results and Discussion

Redox Potentials of 4BRu^{2+} and 5BRu^{2+}. The DBDE group at the 4 or 5 position of the phen ligand in **4BRu**$^{2+}$ or **5BRu**$^{2+}$, respectively, will act as an electron-accepting unit owing to the presence of p(B), and this will reflect on the redox potentials of the complexes. The cyclic voltammograms (CVs) thus observed for **4BRu**$^{2+}$ and **5BRu**$^{2+}$ in DMF are shown in Figure 1 together with that of Ru(phen)$_3^{2+}$ as a reference complex, and the redox potentials of the complexes (vs SCE) are summarized in Table 1. As seen in Figure 1, the CV of Ru(phen)$_3^{2+}$ exhibited a metal oxidation wave (E^{ox}; $E(Ru^{3+/2+})$) and three reduction waves responsible for consecutive one-electron reductions of the three phen ligands ($E^{red(1,2,3)}$; $E(Ru^{2+/+})$, $E(Ru^{+/0})$, and $E(Ru^{0/-})$, respectively).[23] The E^{ox} and $E^{red(1,2,3)}$ values of Ru(phen)$_3^{2+}$ determined in the present study (+1.26, −1.27, −1.42, and −1.74 V in DMF, respectively) corresponded very well to the reported values (+1.35, −1.36, −1.46, and −1.80 V in CH_3CN, respectively).[23b] **4BRu**$^{2+}$ and **5BRu**$^{2+}$ also exhibited one metal oxidation wave and three consecutive reduction waves similar to those of Ru(phen)$_3^{2+}$. The E^{ox} values of **4BRu**$^{2+}$ and **5BRu**$^{2+}$ were almost identical with that of Ru(phen)$_3^{2+}$, with the value of both complexes being +1.28 V, indicating that the introduction of the DBDE group to phen resulted in a minor effect on the E^{ox} value.

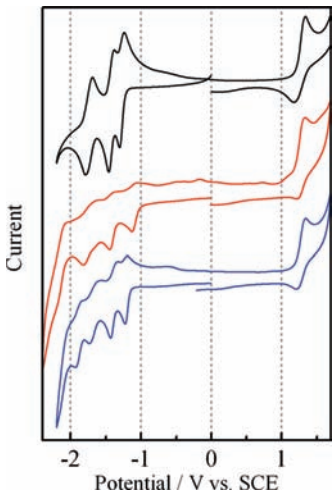

Figure 1. CVs of Ru(phen)$_3^{2+}$ (black), **4BRu**$^{2+}$ (red), and **5BRu**$^{2+}$ (blue) in DMF in the presence of 0.10 M $TBAPF_6$. Scan rate = 100 mV s^{-1}.

Table 1. Redox Potentials of Ru(phen)$_3^{2+}$, **4BRu**$^{2+}$, and **5BRu**$^{2+}$ in DMF (0.1 M $TBAPF_6$)[a]

	potential/V (vs SCE)				
	E^{ox}	$E^{red(1)}$	$E^{red(2)}$	$E^{red(3)}$	$E^{red(4)}$
Ru(phen)$_3^{2+}$	+1.26	−1.27	−1.42	−1.74	
4BRu^{2+}	+1.28	−1.09	−1.41	−1.75	−2.12
4BRu^{2+} + F$^-$ [b]	+1.30	−1.20	−1.43	−1.67	
5BRu^{2+}	+1.28	−1.21	−1.39	−1.68	−1.89
5BRu^{2+} + F$^-$ [b]	+1.30	−1.25	−1.40	−1.71	

[a] [Ru(phen)$^{2+}$] = 1.1×10^{-3} M, [**4BRu**$^{2+}$] = 4.9×10^{-4} M, [**5BRu**$^{2+}$] = 5.4×10^{-4} M, and [F$^-$] = 5.5×10^{-4} M. [b] Data were compiled from Figure S1 in the Supporting Information.

In marked contrast to E^{ox}, the presence of the DBDE group on the phen ligand largely influenced $E^{red(1,2,3)}$ of both **4BRu**$^{2+}$ and **5BRu**$^{2+}$. In the case of **4BRu**$^{2+}$, $E^{red(1)}$ was observed at a more positive potential (−1.09 V) by 180 mV compared with that of Ru(phen)$_3^{2+}$ (−1.27 V), while $E^{red(2,3)}$ (−1.41 and −1.75 V, respectively) agreed very well with the relevant value of Ru(phen)$_3^{2+}$ within ±10 mV. The $E^{red(1)}$ value of **5BRu**$^{2+}$ (−1.21 V) was shifted in the positive direction by 60 mV relative to that of Ru(phen)$_3^{2+}$, while the potential shift by an introduction of the DBDE group to the phen ligand in **5BRu**$^{2+}$ was rather moderate compared with that of **4BRu**$^{2+}$. The $E^{red(2,3)}$ values of **5BRu**$^{2+}$ were also shifted to the positive potential compared with those of **4BRu**$^{2+}$ or Ru(phen)$_3^{2+}$. For both **4BRu**$^{2+}$ and **5BRu**$^{2+}$, furthermore, the fourth reduction waves ($E^{red(4)}$) were observed at −2.12 and −1.89 V, respectively, which was not observed for Ru(phen)$_3^{2+}$.

(21) (a) Suzuki, K.; Kobayashi, A.; Kaneko, S.; Takehira, K.; Yoshihara, T.; Ishida, H.; Shiina, Y.; Oishi, S.; Tobita, S. *Phys. Chem. Chem. Phys.* **2009**, *11*, 9850. (b) Ishida, H.; Tobita, S.; Hasegawa, Y.; Katoh, R.; Nozaki, K. *Coord. Chem. Rev.* **2010**, *254*, 2449.

(22) Frisch, M. J.; Trucks, G. W.; Schlegel, H. B.; Scuseria, G. E.; Robb, M. A.; Cheeseman, J. R.; Scalmani, G.; Barone, V.; Mennucci, B.; Petersson, G. A.; Nakatsuji, H.; Caricato, M.; Li, X.; Hratchian, H. P.; Izmaylov, A. F.; Bloino, J.; Zheng, G.; Sonnenberg, J. L.; Hada, M.; Ehara, M.; Toyota, K.; Fukuda, R.; Hasegawa, J.; Ishida, M.; Nakajima, T.; Honda, Y.; Kitao, O.; Nakai, H.; Vreven, T.; Montgomery, J. A., Jr.; Peralta, J. E.; Ogliaro, F.; Bearpark, M.; Heyd, J. J.; Brothers, E.; Kudin, K. N.; Staroverov, V. N.; Kobayashi, R.; Normand, J.; Raghavachari, K.; Rendell, A.; Burant, J. C.; Iyengar, S. S.; Tomasi, J.; Cossi, M.; Rega, N.; Millam, J. M.; Klene, M.; Knox, J. E.; Cross, J. B.; Bakken, V.; Adamo, C.; Jaramillo, J.; Gomperts, R.; Stratmann, R. E.; Yazyev, O.; Austin, A. J.; Cammi, R.; Pomelli, C.; Ochterski, J. W.; Martin, R. L.; Morokuma, K.; Zakrzewski, V. G.; Voth, G. A.; Salvador, P.; Dannenberg, J. J.; Dapprich, S.; Daniels, A. D.; Farkas, O.; Foresman, J. B.; Ortiz, J. V.; Cioslowski, J.; Fox, D. J. *Gaussian 09*, revision A.1; Gaussian, Inc.: Wallingford, CT, 2009.

(23) (a) Kalyanasundaram, K. *Photochemistry of Polypyridine and Porphyrin Complexes*; Academic Press: London, 1992. (b) Bouskila, A.; Drahi, B.; Amouyal, E.; Sasaki, I.; Gaudemer, A. *J. Photochem. Photobiol. A: Chem.* **2004**, *163*, 381.

To assign the fourth reduction waves observed for **4BRu**$^{2+}$ and **5BRu**$^{2+}$, we studied the effects of a fluoride ion (tetra-*n*-butylammonium fluoride, TBAF) on the redox potentials of the complexes, as shown by the CVs in Figure S1 in the Supporting Information, and the redox potentials of the complexes in the presence of F^- ([TBAF] = 5.5×10^{-4} M) are included in Table 1. It has been reported that triarylboranes and transition-metal complexes bearing a triarylborane unit(s) act as fluoride ion sensors[7,10,11b,11c,12,24] because a F^- ion is likely to coordinate with p(B), and this results in large changes in the redox and absorption/emission properties of the compounds compared with those in the absence of F^-. It is worth noting that a PF_6^- ion used as a supporting electrolyte in the CV experiments (i.e., $TBAPF_6$) or a counter anion of **4BRu**$^{2+}$ or **5BRu**$^{2+}$ cannot bind with p(B) because a PF_6^- ion is too large to access p(B) on the boron atom surrounded by the bulky dimesityl and duryl groups in **4BRu**$^{2+}$ or **5BRu**$^{2+}$. Figure S1 in the Supporting Information and Table 1 clearly demonstrate the disappearance of the $E^{red(4)}$ wave and the negative potential shift of the $E^{red(1)}$ value of **4BRu**$^{2+}$ (−1.20 V) or **5BRu**$^{2+}$ in the presence of F^- (−1.25 V) compared with that in the absence of F^-: −1.09 or −1.21 V, respectively. These results indicate that $E^{red(1)}$ and $E^{red(4)}$ are under the strong influence of p(B). Because the $E^{red(4)}$ wave is not observed in Ru(phen)$_3^{2+}$, the reduction wave could be assigned to that of the DBDE group in **4BRu**$^{2+}$ or **5BRu**$^{2+}$: electron occupation by p(B). Furthermore, the negative potential shift of $E^{red(1)}$ observed for **4BRu**$^{2+}$ or **5BRu**$^{2+}$ in the presence of F^- relative to that in the absence of F^- demonstrates that $E^{red(1)}$ is essentially responsible for the reduction of the phen ligand having the DBDE group in **4BRu**$^{2+}$ or **5BRu**$^{2+}$. The rather insensitive nature of $E^{red(2,3)}$ of **4BRu**$^{2+}$ and **5BRu**$^{2+}$ to F^- indicates that the reduction waves of the complexes are ascribed to the reduction of the phen ligands without DBDE. It is worth emphasizing that the DBDE group introduced to the 4 position of phen shows a stronger electron-accepting ability compared with that to the 5 position of phen. The reduction potentials observed for **4BRu**$^{2+}$ or **5BRu**$^{2+}$, different from those of Ru(phen)$_3^{2+}$, should reflect the spectroscopic and photophysical properties of the complexes, and the results are described in the following sections.

Absorption Spectra of 4BRu^{2+} and 5BRu^{2+}. Figure 2 shows the absorption spectra of the three Ru(II) complexes in CH_3CN at 298 K, and the spectroscopic data are summarized in Table 2: the absorption maximum wavelength (λ^{abs}) and the molar absorption coefficient (ε). The absorption bands of Ru(phen)$_3^{2+}$ at λ^{abs} = 263 and 445 nm have been assigned to the ligand-centered (LC) and MLCT transitions, respectively.[25] Owing to the close similarities of the absorption spectral band shapes and maximum wavelengths of the two main bands of **4BRu**$^{2+}$ (λ^{abs} = 264 and 473 nm) or **5BRu**$^{2+}$ (263 and 448 nm) with those of Ru(phen)$_3^{2+}$, the shorter- and longer-wavelength absorption bands observed for the complexes could be tentatively assigned to the LC ($\pi\pi^*$ transition in phen) and MLCT transitions, respectively. The MLCT absorption band of **4BRu**$^{2+}$ was observed at the lower energy [wavenumber (ν^{abs}) = 21.14×10^3 cm^{-1}] by 1330 cm^{-1} compared with that of Ru(phen)$_3^{2+}$ (ν^{abs} = 22.47×10^3 cm^{-1}). Because the HOMO/LUMO energy gap of **4BRu**$^{2+}$ estimated from the E^{ox} and $E^{red(1)}$ values in Table 1 ($\Delta E = E^{ox} - E^{red(1)}$) is smaller than that of Ru(phen)$_3^{2+}$ by 1290 cm^{-1} and the value agrees very well with the difference in ν^{abs} between **4BRu**$^{2+}$ and Ru(phen)$_3^{2+}$, the lower-energy shift of the MLCT absorption band of **4BRu**$^{2+}$ relative to that of Ru(phen)$_3^{2+}$ will be reasonably explained by the electron-accepting ability of the DBDE group in **4BRu**$^{2+}$. Similarly, the small lower-energy shift of the MLCT band observed for **5BRu**$^{2+}$ (ν^{abs} = 22.32×10^3 cm^{-1}) by 150 cm^{-1} compared with ν^{abs} of Ru(phen)$_3^{2+}$ will also be accounted for by the small ΔE value of the complex relative to that of Ru(phen)$_3^{2+}$: 320 cm^{-1}.

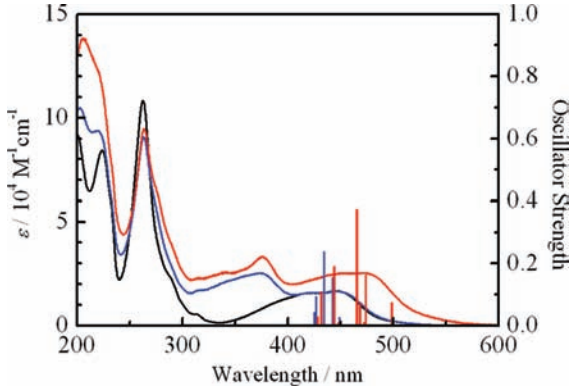

Figure 2. Absorption spectra of Ru(phen)$_3^{2+}$ (black), **4BRu**$^{2+}$ (red), and **5BRu**$^{2+}$ (blue) in acetonitrile at 298 K. The perpendicular bars shown by the red and blue colors represent the oscillator strengths of several absorption transitions in **4BRu**$^{2+}$ and **5BRu**$^{2+}$, respectively. See also Figure 4 and Tables S1 and S2 in the Supporting Information.

Figure 2 also indicates that both **4BRu**$^{2+}$ and **5BRu**$^{2+}$ exhibit a new absorption band in 300−400 nm, not observed for Ru(phen)$_3^{2+}$. It is worth emphasizing that the absorption band similar to that of **4BRu**$^{2+}$ or **5BRu**$^{2+}$ at 300−400 nm can be observed for Ru(phen)$_2$(4-durylethynylphen)$^{2+}$ or Ru(phen)$_2$(5-durylethynylphen)$^{2+}$ (i.e., a **4BRu**$^{2+}$ or **5BRu**$^{2+}$ type complex without a dimesitylboryl group) but not for the ligand itself, as reported in Figure S2 in the Supporting Information. Therefore, the absorption band observed for **4BRu**$^{2+}$ or **5BRu**$^{2+}$ at 300−400 nm is responsible for the Ru(II)-to-π(durylethynylphen) CT transition. Nonetheless, one should

(24) (a) Yamaguchi, S.; Akiyama, S.; Tamao, K. *J. Am. Chem. Soc.* **2001**, *123*, 11372. (b) Yamaguchi, S.; Akiyama, S.; Tamao, K. *J. Organomet. Chem.* **2002**, *652*, 3. (c) Kubo, Y.; Yamamoto, M.; Ikeda, M.; Takeuchi, M.; Shinkaia, S.; Yamaguchi, S.; Tamao, K. *Angew. Chem., Int. Ed.* **2003**, *42*, 2036. (d) Melami, M.; Gabbaï, F. P. *J. Am. Chem. Soc.* **2005**, *127*, 9680. (e) Parab, K.; Venkatasubbaiah, K.; Jäkle, F. *J. Am. Chem. Soc.* **2006**, *128*, 12879. (f) Zhou, Z.; Xiao, S.; Xu, J.; Liu, Z.; Shi, M.; Li, F.; Yi, T.; Huang, C. *Org. Lett.* **2006**, *8*, 3911. (g) Zhou, Z.; Yang, H.; Shi, M.; Xiao, S.; Li, F.; Yi, T.; Huang, C. *ChemPhysChem* **2007**, *8*, 1289. (h) Hudnall, T. W.; Kim, Y.-M.; Bebbington, M. W.; Bourissou, D.; Gabbaï, F. P. *J. Am. Chem. Soc.* **2008**, *130*, 10890. (i) Kim, Y.; Gabbaï, F. P. *J. Am. Chem. Soc.* **2009**, *131*, 3363. (j) Hudson, Z. M.; Wang, S. *Acc. Chem. Res.* **2009**, *42*, 1584. (k) Hudnall, T. W.; Chiu, C.-W.; Gabbaï, F. P. *Acc. Chem. Res.* **2009**, *42*, 388. (l) Wade, C. R.; Broomsgrove, A. E. J.; Aldridge, S.; Gabbaï, F. P. *Chem. Rev.* **2010**, *110*, 3958.

(25) (a) Kalyanasundaram, K. *Coord. Chem. Rev.* **1982**, *46*, 159. (b) Ferguson, J.; Herren, F.; Krausz, E. R.; Vrbancich, J. *Coord. Chem. Rev.* **1985**, *64*, 21. (c) Juris, A.; Barigelletti, F.; Campagna, S.; Balzani, V.; Belser, P.; von Zelewsky, A. *Coord. Chem. Rev.* **1988**, *84*, 85. (d) Wallace, A. W.; Murphy, W. R., Jr.; Petersen, J. D. *Inorg. Chim. Acta* **1989**, *166*, 47.

Table 2. Spectroscopic and Photophysical Properties of $Ru(phen)_3^{2+}$, **4BRu**$^{2+}$, and **5BRu**$^{2+}$ in Acetonitrile at 298 K

	λ^{abs}/nm (ε/10^4 M^{-1} cm^{-1})	λ^{em}/nm	Φ^{em}	τ^{em}/μs	k_r/10^4 s^{-1}	k_{nr}/10^4 s^{-1}
$Ru(phen)_3^{2+}$	263 (11), 445 (1.7)	599	0.045	0.42	11	230
4BRu^{2+}	264 (9.5), 376 (3.3), 473 (2.6)	681	0.11	12	0.92	7.4
5BRu^{2+}	263 (9.1), 373 (2.5), 448 (1.7)	607	0.11	1.2	9.2	74

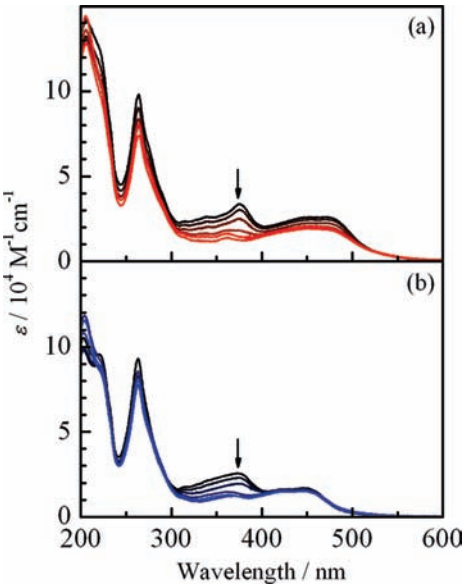

Figure 3. Absorption spectra of **4BRu**$^{2+}$ (a) and **5BRu**$^{2+}$ (b) in the absence and presence of TBAF in acetonitrile at 298 K. TBAF equivalences were 0, 0.47, 0.93, 1.9, 2.8, and 3.7 for **4BRu**$^{2+}$ and 0, 0.49, 0.99, 2.0, and 3.0 for **5BRu**$^{2+}$.

consider the contribution of the DBDE group [i.e., p(B)] to the absorption spectrum of **4BRu**$^{2+}$ or **5BRu**$^{2+}$ similar to that to the redox potentials of the complexes. Therefore, we studied the effects of a F^- ion on the absorption spectra of the complexes.

Figure 3 shows the absorption spectral responses of **4BRu**$^{2+}$ and **5BRu**$^{2+}$ to a F^- ion in CH_3CN: molar concentration ratio of [complex]/[F^-] = 1.0/0−3.7 and 1.0/0−3.0, respectively. As is clearly seen in the figures, the absorption band intensities of both complexes at 300−400 nm decrease in the presence of F^-. This demonstrates that the dimesitylboryl group or p(B) also contributes to the electronic transition(s) at 300−400 nm and, thus, the π-electron system in the durylethynyl group communicates with that of the dimesitylboryl group in **4BRu**$^{2+}$ or **5BRu**$^{2+}$, indicating that the absorption band is ascribed to superposition of the Ru(II)-to-π(durylethynylphen) CT and Ru(II)-to-π(DBDE)/p(B) CT transitions; we define this synergistic MLCT/π(aryl)−p(B) CT interaction. Figure 3 indicates, furthermore, that the presence of p(B) influences the entire electronic absorption transitions in **4BRu**$^{2+}$, while the contribution of p(B) to the MLCT transition of **5BRu**$^{2+}$ is rather small compared with that of **4BRu**$^{2+}$. Thus, the synergistic MLCT/π(aryl)−p(B) CT interactions are stronger in **4BRu**$^{2+}$ than in **5BRu**$^{2+}$. In the case of **4BRu**$^{2+}$, this gives rise to the large ε value of the MLCT transition (2.6×10^4 M^{-1} cm^{-1} at λ^{abs} = 473 nm) relative to that of **5BRu**$^{2+}$ (1.7×10^4 M^{-1} cm^{-1} at λ^{abs} = 448 nm). The results indicate that an introduction of the DBDE group to the phen ligand in **4BRu**$^{2+}$ brings about enhancement of the ε value and the longer-wavelength shift of the MLCT (i.e., MLCT/π(aryl)−p(B)) absorption transition. Furthermore, the present results demonstrate that the position of the DBDE group introduced to phen is a very important factor governing the synergistic MLCT/π(aryl)−p(B) CT interactions and the introduction of the group to the 4 position of phen results in larger effects on the electronic structures of the complex compared with that to the 5 position of phen.

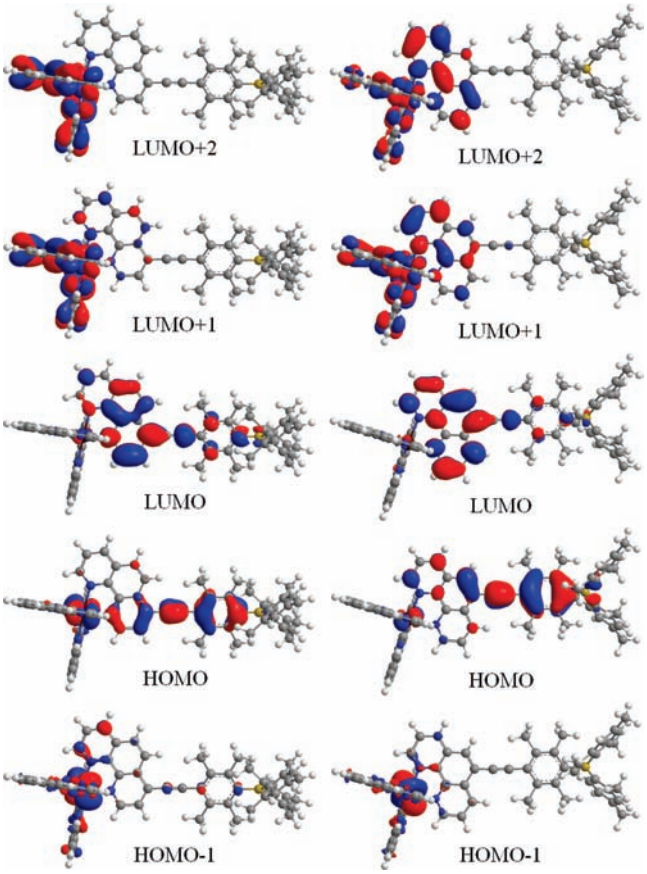

Figure 4. Electron density maps in the HOMO and LUMO levels of **4BRu**$^{2+}$ and **5BRu**$^{2+}$ whose geometries were optimized by the DFT calculations at the B3LYP/6-31* level.

TD-DFT Calculations of the HOMO/LUMO Levels in 4BRu^{2+} and 5BRu^{2+}. To confirm the above discussions, we conducted TD-DFT calculations, as the electron density maps at several HOMO/LUMO levels in **4BRu**$^{2+}$ and **5BRu**$^{2+}$ show in Figure 4. The oscillator strengths (f) of the 10 lowest-energy absorption transitions estimated by the TD-DFT calculations are also included in Figure 2, and the detailed data are reported in Tables S1 and S2 in the Supporting Information. According to our calculations, the lowest-energy absorption transition in **4BRu**$^{2+}$ is ascribed to the HOMO (48%)/HOMO−1 (52%) → LUMO transition at 498.61 nm with f = 0.0744 (see Table S1 in the Supporting Information). The HOMO/

HOMO−1 levels of **4BRu**$^{2+}$ are characterized by the electron densities on the Ru(II) atom and the pyridine ring in the durylethynylphen system without any contribution of p(B) to the HOMOs, while the excited electron in the LUMO distributes to both p(B) and the durylethynylphen system. The results clearly support our assignment of the lowest-energy absorption band of **4BRu**$^{2+}$ to the synergistic MLCT/π(aryl)−p(B) CT. Our calculations on the f values of several transitions in **4BRu**$^{2+}$ also reproduce very well the observed absorption spectrum seen in Figure 2.

In the case of **5BRu**$^{2+}$, on the other hand, the HOMO−1 is described by electron localization on the Ru(II) atom, whereas the electron density in the HOMO distributes to both p(B) and the durylethynylphen group. The LUMO of **5BRu**$^{2+}$ is characterized by the large electron densities in the durylethynylphen ligand with a minor contribution of the density on p(B). The lowest-energy absorption transition predicted for **5BRu**$^{2+}$ is the HOMO−1 → LUMO (47%)/LUMO+2 (53%) transition at 473.92 nm with f = 0.0002 without any contribution of the HOMO level. Because the LUMO+2 level is localized on the Ru(II)-phen core, the π(aryl)−p(B) CT character in the lowest excited state is predicted to be weaker than that in **4BRu**$^{2+}$, which agrees very well with the present observations on both the redox potentials and absorption spectra of **4BRu**$^{2+}$ and **5BRu**$^{2+}$. Furthermore, our calculations reproduced very well the absorption spectrum of **5BRu**$^{2+}$ in Figure 2: see also Table S2 in the Supporting Information. Therefore, the TD-DFT calculations explain very well the present experimental observations, and we conclude that the absorption transitions in both **4BRu**$^{2+}$ and **5BRu**$^{2+}$ are characterized by synergistic MLCT/π(aryl)−p(B) CT interactions, while the contribution of the π(aryl)−p(B) CT is stronger in **4BRu**$^{2+}$ than in **5BRu**$^{2+}$.

Emission Characteristics of 4BRu^{2+} and 5BRu^{2+}. Figure 5 shows the emission spectra of the three Ru(II) complexes in CH_3CN at 298 K, where the emission intensities of the complexes are normalized to those at the maximum wavelengths (λ^{em}). Because the lowest-energy absorption bands of both **4BRu**$^{2+}$ and **5BRu**$^{2+}$ are assigned to the MLCT/π(aryl)−p(B) CT transitions, the emissions from these complexes will also be ascribed to the MLCT-type emissions. In practice, both **4BRu**$^{2+}$ and **5BRu**$^{2+}$ exhibited broad and structureless emissions at λ^{em} = 681 and 607 nm, respectively, similar to Ru(phen)$_3^{2+}$ (λ^{em} = 599 nm). The longer wavelength shift of the emission from **4BRu**$^{2+}$ relative to that from **5BRu**$^{2+}$ or Ru(phen)$_3^{2+}$ is a reasonable consequence, as expected from the λ^{abs} values and the redox potentials of these complexes.

The Φ^{em} and τ^{em} values evaluated for the Ru(II) complexes are included in Table 2. Both **4BRu**$^{2+}$ and **5BRu**$^{2+}$ showed intense emissions with Φ^{em} = 0.11, whose value was almost 2 times larger than that of Ru(phen)$_3^{2+}$: Φ^{em} = 0.045. Furthermore, the τ^{em} values of **4BRu**$^{2+}$ and **5BRu**$^{2+}$ were 12 and 1.2 μs, respectively. Because τ^{em} of Ru(phen)$_3^{2+}$ is 0.42 μs, an introduction of the DBDE group to the 4 or 5 position of the phen ligand gives rise to elongation of τ^{em} by a factor of ∼29 or 2.9, respectively. It is worth noting that the emissions from both **4BRu**$^{2+}$ and **5BRu**$^{2+}$ are quenched by F^-, as the data show in Figure S3 in the Supporting Information. Therefore, the emissive MLCT excited states of these complexes are also under the strong influence of p(B) and, thus, the synergistic MLCT/π(aryl)−p(B) CT interactions. These results explicitly demonstrate that an introduction of the triarylborane CT unit extraordinarily influences the photoophysical properties of the complexes.

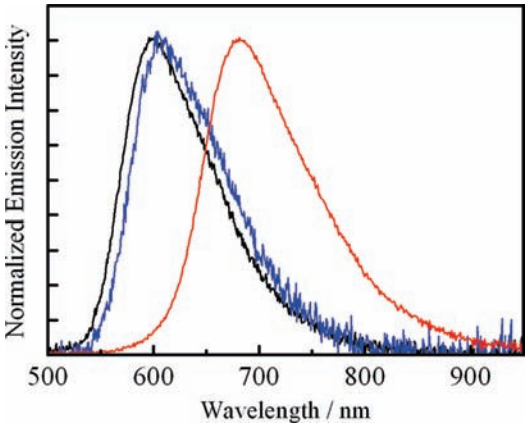

Figure 5. Emission spectra of Ru(phen)$_3^{2+}$ (black), **4BRu**$^{2+}$ (red), and **5BRu**$^{2+}$ (blue) in acetonitrile at 298 K.

Table 2 includes the radiative (k_r) and nonradiative rate constants (k_{nr}) of the three complexes evaluated by the relation $\Phi^{em} = k_r/(k_r + k_{nr}) = k_r\tau^{em}$. The k_r value of **5BRu**$^{2+}$ (9.2×10^4 s^{-1}) was almost comparable to that of Ru(phen)$_3^{2+}$ (11×10^4 s^{-1}), while that of **4BRu**$^{2+}$ (0.92×10^4 s^{-1}) was almost one-tenth of the k_r value of Ru(phen)$_3^{2+}$. Irrespective of the k_r value, however, the k_{nr} value is much larger than k_r for each complex and, thus, the emission lifetimes of these complexes are primarily determined by k_{nr}. As seen in Table 2, the k_{nr} values of the complexes varied dramatically in the sequence of Ru(phen)$_3^{2+}$ (2.3×10^6 s^{-1}) > **5BRu**$^{2+}$ (7.4×10^5 s^{-1}) > **4BRu**$^{2+}$ (7.4×10^4 s^{-1}), and that of **4BRu**$^{2+}$ or **5BRu**$^{2+}$ was ∼31 or 3.1 times smaller, respectively, than that of Ru(phen)$_3^{2+}$. The long emission lifetime of **4BRu**$^{2+}$ or **5BRu**$^{2+}$ is thus essentially responsible for the small k_{nr} value.

The k_{nr} values of Ru(II) or Os(II) complexes have been frequently discussed on the basis of the energy gap law,[2] by which the ln k_{nr} value correlates linearly with the emission maximum energy (ν^{em}) through the relations

$$\ln k_{nr} \propto -\frac{\gamma_0 \nu^{em}}{\hbar\omega} \quad (1)$$

where ω is the angular frequency of the vibration(s) responsible for nonradiative decay and γ_0 is given by

$$\gamma_0 = \ln \frac{\nu^{em}}{S\hbar\omega} - 1 \quad (2)$$

where S is the parameter related to the vibrational displacement between the ground- and excited-state potential surfaces. Although the ν^{em} term is included in γ_0, this contribution to an energy gap plot has been reported to be minor. Therefore, ln k_{nr} should correlate linearly with ν^{em} under the assumption of the energy gap law.[2] Nonetheless, it is clear that the k_{nr} values of **4BRu**$^{2+}$ and **5BRu**$^{2+}$ cannot be explained by the energy gap law

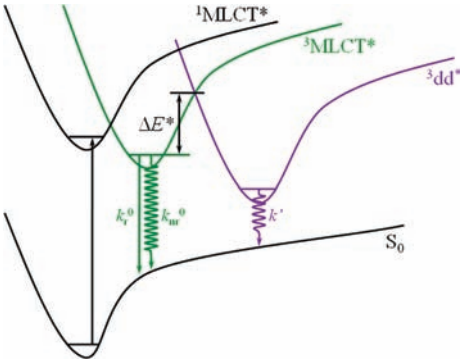

Figure 6. Schematic illustration of the three-state model for the nonradiative decay of a polypyridine ruthenium(II) complex.

because the lower-energy emission from **4BRu**$^{2+}$ (ν^{em} = 14.7×10^3 cm^{-1}) shows a smaller k_{nr} value (7.4×10^4 s^{-1}) compared with k_{nr} of the higher-energy emission from **5BRu**$^{2+}$ ($\nu^{em} = 16.5 \times 10^3$ cm^{-1} and $k_{nr} = 7.4 \times 10^5$ s^{-1}) or Ru(phen)$_3^{2+}$ ($\nu^{em} = 16.7 \times 10^3$ cm^{-1} and $k_{nr} = 2.3 \times 10^6$ s^{-1}). Clearly, one must seek another possible origin of the long emission lifetime or small k_{nr} value of **4BRu**$^{2+}$ other than the energy-gap dependence of k_{nr}.

Temperature Dependences of the Emission Lifetimes of 4BRu^{2+} and 5BRu^{2+}. Another factor governing τ^{em} of a Ru(II) complex in solution at around room temperature is thermal population of the emitting ^{3}MLCT* state to the nonemitting ^{3}dd* state and subsequent fast nonradiative decay from the ^{3}dd* state to the ground state (S_0), as mentioned before: see also Figure 6. Because the ^{3}MLCT*-^{3}dd* interconversion process requires an activation energy (ΔE^* in Figure 6), τ^{em} of Ru(II), in general, decreases with an increase in the temperature (T). According to Van Houten and Watts[3a,b] and Meyer and coworkers,[2,3c] T-dependent τ^{em}, $\tau(T)$, can be given by eq 3

$$\tau(T)^{-1} = ({k_r}^0 + {k_{nr}}^0) + k' \exp\left(-\frac{\Delta E^*}{k_B T}\right) \qquad (3)$$

where ${k_r}^0$ and ${k_{nr}}^0$ are the T-independent k_r and k_{nr} values of the emissive ^{3}MLCT* state, respectively, and k' and k_B are the frequency factor for the ^{3}MLCT*−^{3}dd* interconversion process and the Boltzmann constant, respectively. In the case of Ru(bpy)$_3^{2+}$ as an ordinary Ru(II) showing a large T-dependent τ^{em}, the k' and ΔE^* values in CH_3CN have been reported to be 5.8×10^{13} s^{-1} and 3800 cm^{-1}, respectively.[2a] To reveal the origin of the long τ^{em} value of **4BRu**$^{2+}$, we studied the T dependence of the emission lifetime of **4BRu**$^{2+}$, together with those of **5BRu**$^{2+}$ and Ru(phen)$_3^{2+}$.

Figure 7 shows the emission decay profiles of **4BRu**$^{2+}$ and **5BRu**$^{2+}$ in propylene carbonate in the T range of 280−330 K. For the T-controlled experiments, we employed a high boiling point (bp) and an optically transparent solvent, propylene carbonate (bp = 242 °C), instead of using CH_3CN (bp = 81.6 °C). The data demonstrate that the decay profiles of the complexes obey single-exponential functions irrespective of T. As seen in the figure, τ^{em} of **5BRu**$^{2+}$ depends strongly on T similar to that of Ru(phen)$_3^{2+}$ or Ru(bpy)$_3^{2+}$, whereas that of **4BRu**$^{2+}$ is almost independent of T: 10.7 (280 K) ∼ 9.8 μs (330 K). The T dependences of τ^{em} determined for

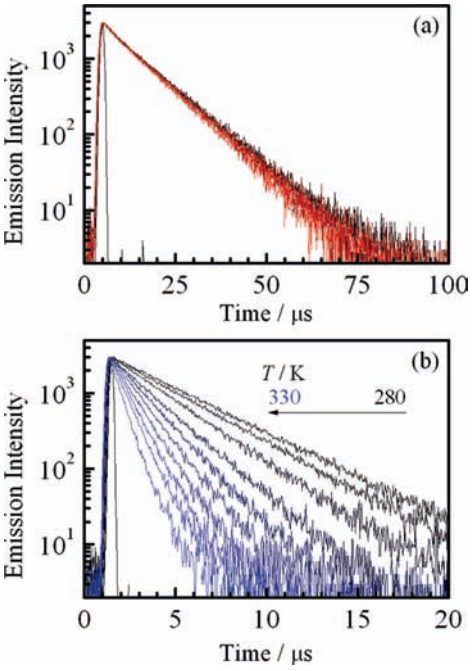

Figure 7. Temperature (T) dependences (280−320 K) of the emission decay profiles of **4BRu**$^{2+}$ (a) and **5BRu**$^{2+}$ (b) in propylene carbonate.

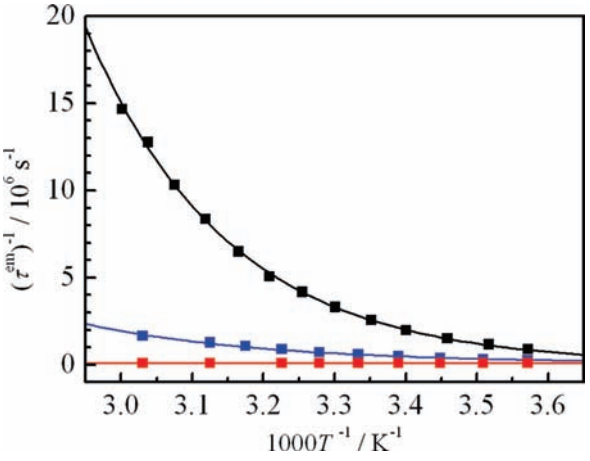

Figure 8. Temperature (T) dependences of the emission lifetimes of Ru(phen)$_3^{2+}$ (black), **4BRu**$^{2+}$ (red), and **5BRu**$^{2+}$ (blue) in propylene carbonate. The solid curves show the best fits by eq 3.

Table 3. Activation Parameters for the ^{3}MLCT*−^{3}dd* Interconversion Process of Ru(phen)$_3^{2+}$, **4BRu**$^{2+}$, and **5BRu**$^{2+}$ in Propylene Carbonate

	ΔE^*/cm^{-1}	k'/s^{-1}	${k_r}^0 + {k_{nr}}^0$/s^{-1}
Ru(phen)$_3^{2+}$	3500	5.7×10^{13}	1.5×10^4
4BRu^{2+}	410	2.1×10^5	6.8×10^4
5BRu^{2+}	2800	2.6×10^{11}	9.9×10^4

4BRu^{2+}, **5BRu**$^{2+}$, and Ru(phen)$_3^{2+}$ are summarized in Figure 8. The solid curves shown in Figure 8 are the best fits of the $\tau(T)$ data by eq 3, and the parameters determined by the fittings are shown in Table 3. The τ^{em} data of Ru(phen)$_3^{2+}$ could be fitted with $k' = 5.7 \times 10^{13}$ s^{-1} and $\Delta E = 3500$ cm^{-1}, whose values were almost comparable to the relevant value of Ru(bpy)$_3^{2+}$ mentioned before. The k' and ΔE^* values of **5BRu**$^{2+}$ were determined to be 2.6×10^{11} s^{-1} and 2800 cm^{-1}, respectively. Although the values determined for **5BRu**$^{2+}$ are somewhat smaller than

the relevant value of $Ru(phen)_3^{2+}$, it will be concluded that the ^{3}MLCT* state of $Ru(phen)_3^{2+}$ or **5BRu**$^{2+}$ undergoes nonradiative decay through the ^{3}dd* state similar to that of $Ru(bpy)_3^{2+}$.[2a] On the other hand, analysis of the τ^{em} data on **4BRu**$^{2+}$ in Figure 8 afforded k' and ΔE as 2.1×10^5 s^{-1} and 410 cm^{-1}, respectively. Clearly, these values are too small to ascribe to the parameters for thermal activation from ^{3}MLCT* to the ^{3}dd* state, and the ΔE value is rather close to the value corresponding to the T dependence of the viscosity in propylene carbonate: 600 cm^{-1}.[26] Therefore, we conclude that the ^{3}dd* state does not participate in nonradiative decay in the ^{3}MLCT* state of **4BRu**$^{2+}$.

It is worth emphasizing that the E^{ox} values of **4BRu**$^{2+}$ and **5BRu**$^{2+}$ are the same at +1.28 V and are comparable to that of $Ru(phen)_3^{2+}$ (+1.26 V), suggesting that the ligand-field-splitting energies of the three complexes are approximately similar to one another and, thus, the ^{3}dd* energies of the complexes will also be similar, although this is a very crude approximation. Nevertheless, **4BRu**$^{2+}$ shows the T-independent τ^{em}, while the τ^{em} values of **5BRu**$^{2+}$ and $Ru(phen)_3^{2+}$ are dependent on T. Because the emission energy of **4BRu**$^{2+}$ is lower than that of **5BRu**$^{2+}$ or $Ru(phen)_3^{2+}$ by 1800−2000 cm^{-1}, one possible explanation for the results on **4BRu**$^{2+}$ in Figure 8 will be the large ^{3}MLCT*−^{3}dd* energy gap, which inhibits thermal activation from ^{3}MLCT* to ^{3}dd*. Without nonradiative decay via the ^{3}dd* state, therefore, the emission lifetime of **4BRu**$^{2+}$ becomes as long as 12 μs in CH_3CN at 298 K. It has been reported that some polypyridine ruthenium(II) complexes show T-independent τ^{em} values similar to that of **4BRu**$^{2+}$, with the represented examples being Ru(II) complexes having 3,3′-bipyridazine,[4d] 2,2′-bipyrazine,[4a] 2,2′-bipyrimidine,[4a,f] and so forth as a ligand(s).[4b,c,g−i] For these complexes, however, because the ^{3}MLCT* states lie in relatively low energy compared with that of $Ru(phen)_3^{2+}$ or $Ru(bpy)_3^{2+}$, very fast nonradiative decay to the ground state occurs as predicted by the energy-gap dependence of k_{nr}, and this gives rise to short τ^{em} values of the complexes.[2] Therefore, **4BRu**$^{2+}$ showing a long-lived, T-independent, and low-energy emission is quite rare.

Implication to the Excited States of Ru(II) Complexes Bearing a 4-Arylethynylphen Ligand. As a Ru(II) complex analogous to **4BRu**$^{2+}$, Glazer et al. reported the dual-emission behavior of $[Ru(bpy)_2\{4\text{-}(4'\text{-R-phenylethynyl})phen\}]^{2+}$ in CH_3CN at room temperature, with the long and short emission lifetime components of the complex with R = −H, −OCH_3, or −CF_3 being 6.6 and 1.2, 11.5 and 1.1, or 6.6 and 1.3 μs, respectively.[27] According to Glazer et al., the origin of the dual emission from the complex is due to participation of the spatially isolated Ru(II)-to-{4-(4′-R-phenylethynyl)phen} and Ru(II)-to-bpy CT excited states, and the long and short emission lifetime components of the complex are ascribed to the former and latter excited states, respectively.[28] They also reported that the long emission lifetime component of $[Ru(bpy)_2\{4\text{-(phenylethynyl)phen}\}]^{2+}$ is not ascribed to the emission from the $\pi\pi^*$ excited triplet state of the 4-(phenylethynyl)phen ligand itself in the complex. We also confirmed that no long-lifetime transient responsible for the $\pi\pi^*$ excited triplet state of the ligand in **4BRu**$^{2+}$ could be observed in nanosecond transient absorption spectroscopy. Thus, the Ru(II)-to-{4-(4′-R-phenylethynyl)phen} CT excited state of such a complex possesses a very long emission lifetime: 6.6−11.5 μs. It is worth noting that $Ru(phen)_2\{4\text{-(durylethynyl)phen}\}^{2+}$ as a reference compound of **4BRu**$^{2+}$ without a dimesitylboryl group in CH_3CN at 298 K shows a single-exponential decay with τ^{em} = 5.8 μs (λ^{em} = 675 nm and Φ^{em} = 0.056). These results indicate that extension of the ligand π-electron system through the arylacetylene unit at the 4 position of phen can elongate the emission lifetime of the relevant Ru(II) complex. Nevertheless, the τ^{em} value of $Ru(phen)_2\{4\text{-(durylethynyl)phen}\}^{2+}$ is almost half of that of **4BRu**$^{2+}$, demonstrating the important role of the synergistic MLCT/π(aryl)−p(B) CT in determining the τ^{em} value of **4BRu**$^{2+}$. Further detailed photophysical studies on the complexes, including low-temperature experiments, are absolutely necessary to explain the excited states of both **4BRu**$^{2+}$ and **5BRu**$^{2+}$, which are now in progress in our laboratory.

Conclusions

In the present study, we demonstrated that **4BRu**$^{2+}$ showed a low-energy emission (λ_{em} = 681 nm and ν_{em} = 14.7×10^3 cm^{-1}) with a long (12 μs in CH_3CN at 298 K) and T-independent emission lifetime (10.7−9.8 μs in 280−330 K) in solution. Although the low-energy and long-lived emission properties of a polypyridin eruthenium(II) complex are mutually contradicting issues as predicted by the energy-gap dependence of k_{nr}, it has been shown by the present study that introduction of a triarylborane CT unit to the 4 position of one of the three phen ligands in $Ru(phen)_3^{2+}$ (i.e., **4BRu**$^{2+}$) fulfills both requirements through participation of the synergistic MLCT/π(aryl)−p(B) CT interactions in the excited state. The synergistic CT interactions in **4BRu**$^{2+}$ can also enhance the MLCT-type absorption intensity in the visible region. Because the complex exhibits a strong redox ability similar to that of $Ru(phen)_3^{2+}$ or $Ru(bpy)_3^{2+}$, **4BRu**$^{2+}$ with the long-lived emission will serve as a good photosensitizer/photocatalyst in solar energy conversion systems.

(26) There are some arguments on the origin of the small but finite activation energy for the relatively small T-dependent emission lifetime of RuL_3^{2+} or $RuL_nL'_{3-n}^{2+}$ where L and L′ are polypyridine ligands. These are (1) participation of a fourth MLCT excited state, (2) T dependence of k_{nr}^0 owing to a T dependence of the emission energy, and (3) nonradiative decay through the higher-energy-lying Ru−L′ MLCT state other than that from the lower-energy-lying Ru−L MLCT state. See also refs 4a and 4f in detail. Alternatively, furthermore, the small ΔE values reported for several Ru(II) complexes have been discussed in terms of zero-field splitting (ZFS) of the emissive MLCT excited triplet state (Barigelletti, F.; Belser, P.; von Zelewsky, A.; Juris, A.; Balzani, V. *J. Phys. Chem.* **1985**, *89*, 3680 and ref 3d). In the present experiments, because the T range studied is rather high (280−330 K) compared with those reported by Barigelletti et al., the discussion on the role of ZFS in ΔE is very difficult. Nevertheless, we suppose that the ΔE value (410 cm^{-1}) observed for **4BRu**$^{2+}$ will be too large to ascribe to the ZFS energy of the emissive excited state.

(27) Glazer, E. C.; Magde, D.; Tor, Y. *J. Am. Chem. Soc.* **2007**, *129*, 8544.

(28) Glazer et al. also reported the dual-emission behavior of a dinuclear Ru(II) complex of $[(bpy)_2Ru\{\mu\text{-(bis-4-phenanthryl)ethyne}\}Ru(bpy)_2]^{4+}$ in solution at room temperature (Glazer, E. C.; Magde, D.; Torr, Y. *J. Am. Chem. Soc.* **2005**, *127*, 4190). We recently confirmed that the absorption/emission spectra and dual-emission behavior of the complex mentioned above could be very well reproduced by our own experiments. Thus, the dual-emission behavior of the Ru(II) complexes having 4-ethynylphen-type ligands reported by Glazer et al. will not be due to emissive impurities of the complexes.

Modulation of the absorption and emission characteristics of $Ru(phen)_3^{2+}$ by introduction of the arylborane CT unit to phen is not fortuitous because $[Pt(B\text{-}tpy)Cl]^+$ mentioned before also shows intense emission with long τ^{em} at room temperature compared with $[Pt(tpy)Cl]^+$ without a triarylborane CT unit.[7] Quite recently, furthermore, we reported that a cyclometalated 2-phenylpyridine (ppy) Ir(III) complex bearing a triarylborane group on ppy, tris[2-{3-(dimesitylboryl)phenyl}pyridinato]iridium(III), showed a bright-green emission with $\Phi^{em} \sim 1.0$ and $\tau^{em} = 1.2$ μs in THF, whose values exceeded the relevant value of $Ir(ppy)_3$ determined under analogous conditions.[29] Several research groups have also reported intense emission from metal complexes having a triarylborane group(s) as described before.[10a,b,11,13] A combination of MLCT and π(aryl)−p(B) CT interactions in a transition-metal complex has thus high potentials to modulate the spectroscopic and photophysical properties of the complex, and a study along the lines mentioned above will open various possibilities of developing potential photosensitizers/photocatalysts in solar energy conversion systems.

Acknowledgment. E.S. and A.I. acknowledge the Global COE program of Hokkaido University (Catalysis as the Basis for Materials Innovation) for a postdoctoral fellowship (2009) and a research fellowship, respectively. E.S. also thanks the F3 Project of MEXT, Japan (2010).

Supporting Information Available: Synthesis of EDDB, purification of other chemicals, details of the TD-DFT calculations, CVs and emission spectra of **4BRu**$^{2+}$ and **5BRu**$^{2+}$ in the absence and presence of TBAF, and absorption spectra of the reference complexes without an arylborane CT unit. This material is available free of charge via the Internet at http://pubs.acs.org.

(29) Ito, A.; Hirokawa, T.; Sakuda, E.; Kitamura, N. *Chem. Lett.* **2011**, *40*, 34.